Ultraviolet and infrared excess emission in Be stars

P. S. Goraya *Uttar Pradesh State Observatory, Manora Peak, Naini Tal – 263 129, India*

Summary. Spectrophotometric observations of 26 Be stars are reported and analysed in the wavelength range $\lambda3200$ to $\lambda8000$ Å. Two observational features readily noted in these stars are: (i) a Balmer discontinuity smaller than that exhibited by normal B-type stars of similar spectral type; and (ii) an excess flux in the near-infrared region. A simple optically thin model is assumed which describes the small Balmer jump as due to free–bound emission in the Balmer continuum arising in a circumstellar envelope. The same model parameters also reproduce the near-infrared excess when Paschen free–free and Paschen free–bound emissions are invoked. The volume emission measures for the circumstellar region are calculated. It is found that the near-ultraviolet and the near-infrared volume emission measures are loosely correlated to each other. The value of the ratio of the Balmer emission measure, ε_{UV}, to the Paschen emission measure, ε_{IR}, is found to be equal to unity.

1 Introduction

The Be stars have drawn the attention of a large number of astronomers in the recent years. This is because of the many associated, interesting and unusual features. The ultraviolet excess emission in Be stars has been found by many authors (Barbier & Chalonge 1941; Mendoza 1958; Schild *et al.* 1974; Schild 1976, 1978). It has also been well established that many Be stars possess infrared excess emission. Johnson's (1967) observations, which revealed the infrared excess of Be stars, were fully confirmed by subsequent observations, including those of Feinstein (1968), Erro (1969), Woolf, Stein & Strittmatter (1970), Allen (1973), Gehrz, Hackwell & Jones (1974), Schild *et al.* (1974), Schild (1976, 1978), Goraya (1980, 1981, 1984a, b), Bhatt *et al.* (1984), etc.

   All these observations show that the majority of Be stars exhibit an extra-photospheric component in their ultraviolet and infrared radiation, which varies in magnitude from star to star. The correlation between the presence of emission lines in the spectrum and the observed infrared excess suggests that all these extra-photospheric features might originate in the same region of the envelope surrounding the star (Feinstein & Marraco 1981; Neto & de Freitas Pacheco 1982;

Dachs & Wamsteker 1982; Feinstein 1982; Ashok *et al.* 1984; Goraya & Rautela 1985). Since the ultraviolet excess and the infrared excess originate from the same envelope, it is interesting to investigate if any correlation exists between them. Such an investigation demands simultaneous ultraviolet and infrared observations because many Be stars exhibit variations in their continuum.

This paper deals with the quantitative analysis of the simultaneous observations of the continuum from the near-ultraviolet to near-infrared region ($\lambda\lambda 3200$–8000 Å). In the present work we have selected only those bright stars, from our extensive spectrophotometric observing programme of Be stars, which possess both near-ultraviolet and near-infrared excess emissions.

2 Observations and reduction

The observations of the programme stars were made on many nights between 1980–83 with the 52-cm and 104-cm reflectors of the observatory. The instrumentation used for taking observations has been described earlier (Goraya 1984a). The Hilger and Watts monochromator with an exit slit giving a 50-Å passband was used for obtaining the continuous spectrum scans of Be stars. The observations were secured in the wavelength range $\lambda\lambda 3200$–8000 Å. Each star was observed many times during a night and the free-hand continuum was drawn through each scan. Each scan was reduced to instrumental magnitudes separately. The instrumental magnitudes were measured at an interval of 100 Å over the entire continuum. All scans of an individual star during a night were averaged to find mean instrumental magnitudes at different wavelengths separated by 100 Å.

Along with the Be Stars, the standard stars α Leo, γ Gem and ξ^2 Cet were also observed many times during a night for the purpose of applying extinction corrections and also to convert instrumental magnitudes of Be stars into absolute magnitudes. Our standardized magnitudes of Be stars correspond to the absolute calibration system of Tug, White & Lockwood (1977). The standard deviation of the measurements on an individual night does not exceed ± 0.03 magnitude in the entire wavelength range. The standardized original observed magnitudes are tabulated in Table 1 along with the date of observations of each star. All the present observations are the mean of observations during a single night.

3 The interstellar reddening for Be stars

The determination of interstellar reddening for Be stars is complicated due to their high rotational velocities and peculiar atmospheric structure. Rapid rotation introduces an intrinsic reddening which is significant for the rapidly rotating Be stars. Neglecting this effect yields an overestimate of interstellar reddening which in turn yields an over-correction of ultraviolet fluxes resulting in a spurious ultraviolet excess. Briot (1978) has found that an ultraviolet flux excess for B0e stars is related to an overestimate of interstellar reddening corrections. Recently, Llorente de Andres *et al.* (1981) have also shown that rapid stellar rotation introduces an additional reddening (intrinsic rotational reddening) which produces an overestimate of the corrections for interstellar extinction. This overestimate of the reddening correction results in the ultraviolet flux excess observed for many Be stars.

The direct measurements of $E(B-V)$ neglect the effect of intrinsic reddening in Be stars. The normal Q method of Johnson & Morgan (1953), valid for the main sequence O and B stars, is likely to give high values of colour excess, $E(B-V)$, because of the ultraviolet and infrared excess emissions in many Be stars.

In order to account for intrinsic rotational reddening and the effect of excess emissions in Be stars, we have used the distance moduli method (*cf.* Goraya 1985) for the determination of colour excess, $E(B-V)$, of Be stars. To determine interstellar reddening, we plotted colour excess, $E(B-$

Table 1. Standardized original observed monochromatic magnitudes of Be stars of the present study.

Wavelength	$1/\lambda$ (μm^{-1})	20 Nov.82 HR 1204	20 Nov.82 HR 1305	19 Nov.82 HR 1763	19 Nov.82 HR 1820	20 Nov.82 HR 2418	16 Oct.80 HR 2745
		m	m	m	m	m	m
3200	3.13	5.784	5.992	5.070	6.154	5.995	4.335
3300	3.03	5.744	5.963	5.398	6.204	6.089	4.462
3400	2.94	5.760	5.963	5.430	6.273	6.036	4.490
3500	2.86	5.740	5.915	5.474	6.278	5.995	4.479
3600	2.78	5.717	5.900	5.531	6.253	5.979	4.514
3700	2.70	5.650	5.882	5.565	6.287	6.000	4.530
3800	2.63	5.200	5.555	5.515	6.135	5.465	4.324
3900	2.56	4.780	5.315	5.440	6.080	5.285	4.190
4000	2.50	4.731	5.312	5.446	6.102	5.267	4.192
4100	2.44	4.690	5.343	5.480	6.105	5.286	4.234
4200	2.38	4.703	5.363	5.504	6.130	5.311	4.263
4300	2.33	4.724	5.385	5.532	6.163	5.325	4.285
4400	2.27	4.773	5.399	5.549	6.190	5.358	4.318
4500	2.22	4.800	5.435	5.587	6.173	5.385	4.367
4600	2.17	4.826	5.448	5.612	6.220	5.400	4.389
4700	2.13	4.835	5.470	5.624	6.253	5.410	4.436
4800	2.08	4.860	5.517	5.663	6.258	5.453	4.446
4900	2.04	4.893	5.527	5.663	6.295	5.453	4.533
5000	2.00	4.912	5.553	5.705	6.310	5.490	4.522
5100	1.96	4.930	5.576	5.707	6.315	5.506	4.434
5200	1.92	4.947	5.590	5.727	6.350	5.540	4.583
5300	1.89	4.984	5.631	5.769	6.368	5.561	4.648
5400	1.85	5.002	5.645	5.767	6.373	5.561	4.641
5500	1.82	5.030	5.665	5.795	6.405	5.586	4.660
5600	1.79	5.060	5.697	5.822	6.413	5.622	4.693
5700	1.75	5.066	5.702	5.855	6.417	5.645	4.726
5800	1.72	5.101	5.748	5.876	6.463	5.653	4.725
5900	1.69	5.120	5.758	5.875	6.500	5.670	4.748
6000	1.67	5.130	5.780	5.913	6.517	5.699	4.770
6100	1.64	5.146	5.800	5.930	6.510	5.719	4.796
6200	1.61	5.140	5.833	5.941	6.526	5.743	4.822
6300	1.59	5.163	5.840	5.964	6.523	5.766	4.825
6400	1.56	5.155	5.864	5.965	6.523	5.795	4.840
6500	1.53	5.183	5.884	5.977	6.545	5.819	4.869
6600	1.51	5.220	5.896	5.995	6.560	5.806	4.984

P. S. Goraya

Table 1 – *continued*

Wavelength	1/λ (μm⁻¹)	20 Nov.82 HR 1204	20 Nov.82 HR 1305	19 Nov.82 HR 1763	19 Nov.82 HR 1820	20 Nov.82 HR 2418	16 Oct.80 HR 2745
		m	m	m	m	m	m
6700	1.49	5.210	5.880	5.973	6.529	5.873	5.944
6800	1.47	5.232	5.915	5.991	6.550	5.825	4.954
6900	1.45	5.255	5.918	5.972	6.588	5.847	4.961
7000	1.43	5.275	5.945	5.988	6.565	5.838	4.979
7100	1.41	5.266	5.972	5.998	6.558	5.873	5.010
7200	1.39	5.287	5.987	6.025	6.576	5.861	5.013
7300	1.37	5.277	5.980	6.022	6.599	5.910	5.066
7400	1.35	5.318	6.010	6.080	6.629	5.904	5.096
7500	1.33	5.323	5.998	6.084	6.675	5.908	5.129
7600	1.32	5.355	6.030	6.100	6.684	5.934	5.136
7700	1.30	5.357	6.089	6.125	6.725	5.970	5.140
7800	1.28	5.396	6.084	6.110	6.715	5.983	5.130
7900	1.27	5.418	6.134	6.131	6.761	6.028	5.150
8000	1.25	5.443	6.160	6.130	6.798	6.050	5.152

Wavelength (Å)	1/λ (μm⁻¹)	10 Dec.82 HR 3034	5 April 81 HR 6118	5 April 81 HR 6873	16 April 81 HR 6881	16 April 81 HR 6984	2 May 83 HR 7318
3200	3.13	4^m.560	–	6^m.265	6^m.556	6^m.169	5^m.475
3300	3.03	4.487	–	6.282	6.516	6.217	5.533
3400	2.94	4.450	–	6.275	6.461	6.245	5.570
3500	2.86	4.462	5^m.280	6.297	6.479	6.222	5.511
3600	2.78	4.473	5.311	6.320	6.440	6.255	5.575
3700	2.70	4.631	5.161	6.362	6.409	6.282	5.568
3800	2.63	4.549	5.036	6.065	5.946	5.879	5.496
3900	2.56	4.480	4.929	5.931	5.719	5.780	5.422
4000	2.50	4.425	4.835	5.910	5.675	5.748	5.414
4100	2.44	4.390	4.810	5.936	5.668	5.768	5.423
4200	2.38	4.420	4.760	5.950	5.667	5.800	5.437
4300	2.33	4.420	4.705	5.970	5.670	5.810	5.417
4400	2.27	4.427	4.687	5.983	5.675	5.850	5.453
4500	2.22	4.445	4.650	5.993	5.666	5.878	5.477
4600	2.17	4.430	4.601	6.010	5.696	5.880	5.440
4700	2.13	4.455	4.596	6.040	5.690	5.918	5.433
4800	2.08	4.430	4.548	6.055	5.697	5.945	5.455

Table 1 – *continued*

Wavelength (Å)	$1/\lambda$ (μm^{-1})	10 Dec.82 HR 3034	5 April 81 HR 6118	5 April 81 HR 6873	16 April 81 HR 6881	16 April 81 HR 6984	2 May 83 HR 7318
		m	m	m	m	m	m
4900	2.04	4.444	4.543	6.075	5.711	5.950	5.455
5000	2.00	4.453	4.498	6.085	5.695	5.987	5.433
5100	1.96	4.453	4.486	6.090	5.711	6.005	5.458
5200	1.92	4.456	4.447	6.132	5.729	6.020	5.451
5300	1.89	4.477	4.403	6.141	5.717	6.042	5.448
5400	1.85	4.460	4.390	6.138	5.725	6.080	5.454
5500	1.82	4.488	4.395	6.158	5.725	6.098	5.450
5600	1.79	4.482	4.358	6.181	5.730	6.111	5.453
5700	1.75	4.507	4.318	6.193	5.722	6.150	5.485
5800	1.72	4.532	4.291	6.222	5.761	6.152	5.394
5900	1.69	4.528	4.292	6.215	5.773	6.200	5.476
6000	1.67	4.556	4.290	6.247	5.786	6.215	5.505
6100	1.64	4.590	4.294	6.294	5.776	6.230	5.508
6200	1.61	4.623	4.304	6.283	5.784	6.243	5.535
6300	1.59	4.632	4.280	6.275	5.764	6.257	5.535
6400	1.56	4.622	4.260	6.305	5.770	6.285	5.545
6500	1.53	4.620	4.280	6.336	5.758	6.320	5.582
6600	1.51	4.620	4.240	6.360	5.775	6.347	5.570
6700	1.49	4.599	4.260	6.356	5.748	6.358	5.566
6800	1.47	4.610	4.238	6.385	5.766	6.376	5.547
6900	1.45	4.636	4.183	6.412	5.766	6.381	5.561
7000	1.43	4.644	4.142	6.418	5.750	6.399	5.570
7100	1.41	4.681	4.087	6.447	5.757	6.420	5.549
7200	1.39	4.697	4.116	6.450	5.742	6.416	5.571
7300	1.37	4.745	4.058	6.455	5.765	6.412	5.537
7400	1.35	4.737	4.080	6.460	5.790	6.425	5.548
7500	1.33	4.753	4.059	6.494	5.820	6.455	5.592
7600	1.32	4.784	4.038	6.510	5.800	6.446	5.570
7700	1.30	4.770	4.010	6.524	5.792	6.490	5.585
7800	1.28	4.759	3.994	6.532	5.858	6.484	5.590
7900	1.27	4.753	3.970	6.504	5.895	6.491	5.615
8000	1.25	4.748	3.960	6.582	5.925	6.521	5.656

126   *P. S. Goraya*

Table 1 – *continued*

Wavelength	$1/\lambda\ (\mu m^{-1})$	2May83 HR 7403	12May83 HR 7418	12May83 HR 7446	28Nov.81 HR 7983	28Nov.81 HR 8047	19Nov.80 HR 8146	4Nov.80 HR 8520
		m	m	m	m	m	m	m
3200	3.13	6.135	5.715	4.915	6.600	4.495	4.185	5.007
3300	3.03	6.117	5.713	4.887	6.595	4.275	4.189	5.040
3400	3.94	6.125	5.676	4.937	6.548	4.295	4.215	5.012
3500	2.86	6.165	5.735	4.937	6.515	4.273	4.176	4.985
3600	2.78	6.175	5.729	4.975	6.500	4.332	4.183	4.970
3700	2.70	6.175	5.522	5.042	6.566	4.455	4.275	4.965
3800	2.63	6.110	5.160	5.013	6.240	4.427	4.165	4.927
3900	2.56	5.983	4.965	4.962	6.104	4.326	4.020	4.780
4000	2.50	5.988	4.892	5.004	6.074	4.320	4.050	4.724
4100	2.44	6.021	4.870	4.946	6.092	4.355	4.063	4.735
4200	2.38	6.055	4.883	4.948	6.094	4.382	4.080	4.770
4300	2.33	6.065	4.917	4.965	6.125	4.405	4.105	4.797
4400	2.27	6.097	4.948	4.945	6.150	4.405	4.120	4.791
4500	2.22	6.135	4.965	4.968	6.159	4.463	4.153	4.829
4600	2.17	6.160	4.990	4.947	6.167	4.480	4.177	4.853
4700	2.13	6.170	5.010	4.955	6.197	4.507	4.208	4.883
4800	2.08	6.210	5.033	4.958	6.207	4.532	4.225	4.851
4900	2.04	6.214	5.076	4.955	6.242	4.560	4.235	4.860
5000	2.00	6.246	5.080	4.954	6.230	4.582	4.257	4.909
5100	1.96	6.275	5.112	4.941	6.262	4.615	4.385	4.914
5200	1.92	6.288	5.122	4.931	6.280	4.627	4.340	4.928
5300	1.89	6.340	5.135	4.952	6.285	4.703	4.348	4.935
5400	1.85	6.362	5.160	4.927	6.320	4.678	4.360	4.965
5500	1.82	6.370	5.177	4.935	6.325	4.703	4.393	4.970
5600	1.79	6.403	5.196	4.959	6.357	4.725	4.410	4.979
5700	1.75	6.417	5.235	4.950	6.368	4.770	4.435	4.978
5800	1.72	6.449	5.232	4.946	6.374	4.802	4.462	4.989
5900	1.69	6.483	5.252	4.965	6.405	4.810	4.477	4.995
6000	1.67	6.492	5.260	4.974	6.430	4.818	4.509	5.008
6100	1.64	6.529	5.377	4.961	6.450	4.848	4.501	4.986
6200	1.61	6.530	5.284	4.972	6.447	4.862	4.490	5.008
6300	1.59	6.575	5.310	5.001	6.490	4.870	4.523	5.021
6400	1.56	6.600	5.328	4.991	6.512	4.875	4.540	5.025
6500	1.53	6.625	5.348	5.003	6.507	4.925	4.581	5.006
6600	1.51	6.625	5.362	5.024	6.516	4.966	4.575	5.032

Table 1 – *continued*

Wavelength	$1/\lambda$ (μm^{-1})	2May83 HR 7403	12May83 HR 7418	12May83 HR 7446	28Nov.81 HR 7983	28Nov.81 HR 8047	19Nov.80 HR 8146	4Nov.80 HR 8520
		m	m	m	m	m	m	m
6700	1.49	6.629	5.360	5.005	6.523	4.995	4.582	5.062
6800	1.47	6.645	5.395	5.024	6.532	4.985	4.585	5.070
6900	1.45	6.680	5.413	5.032	6.550	5.032	4.602	5.057
7000	1.43	6.677	5.418	5.040	6.530	5.012	4.639	5.101
7100	1.41	6.700	5.416	5.044	6.563	5.057	4.647	5.124
7200	1.39	6.710	5.552	5.047	6.595	5.108	4.663	5.130
7300	1.37	6.712	5.475	5.066	6.615	5.105	4.676	5.171
7400	1.35	6.755	5.500	5.049	6.608	5.092	4.677	5.151
7500	1.33	6.754	5.513	5.015	6.651	5.091	4.679	5.129
7600	1.32	6.774	5.513	5.034	6.680	5.129	4.675	5.143
7700	1.30	6.822	5.526	5.006	6.673	5.134	4.680	5.170
7800	1.28	6.816	5.523	5.092	6.700	5.116	4.687	5.153
7900	1.27	6.855	5.522	5.100	6.735	5.113	4.671	5.125
8000	1.25	6.922	5.530	5.154	6.780	5.119	4.659	5.135

V), of about 60–100 normal B stars lying in the direction of each programme Be star, against their apparent distance moduli ($m_V - M_V$). The $E(B-V)$ values for normal B stars were computed through the Q method. The normal B stars were selected from the *Photoelectric Catalogue* (Blanco *et al.* 1968). To estimate the apparent distance moduli of normal B stars the M_V magnitudes were taken from the spectral type and luminosity class versus M_V calibration for early-type stars (Allen 1976). From the distance moduli versus $E(B-V)$ plot for normal B stars, the $E(B-V)$ values of programme Be stars corresponding to their distance moduli were estimated. The $E(B-V)$ values thus estimated are listed in Table 2(a). The reddening at visual magnitudes (A_V) was derived by adopting a mean value of total-to-selective extinction, $R=3.25$ (Moffat & Schmidt-Kaler 1976). The reddening at visual magnitude is given in Table 2(a). The reddening corrections were calculated at different wavelengths by adopting these values of A_V and using the reddening law given by Lucke (1980). Since the reddening law by Lucke (1980) is available only in the wavelength range $\lambda\lambda 3200$–6000 Å, this reddening law was extrapolated to $\lambda 8000$ Å with the help of the reddening law given by Schild (1977).

The standardized observed magnitudes listed in Table 1 were corrected for interstellar reddening by using the distance moduli method described above. The dereddened magnitudes normalized to wavelength $\lambda 5500$ Å are tabulated in Table 2(b) along with the adopted values of reddening corrections. The dereddened energy distributions of Be stars were compared with theoretical models (Kurucz 1979) to find the effective temperature of these stars. For deriving the effective temperature of Be stars we compared the $\lambda\lambda 4000$–5500 Å region of the observed continuum energy distribution with the theoretical energy distribution because this region of the continuum is not affected by excess emissions from the envelope (Goraya 1985). We assumed $\log g = 4.0$ for luminosity class IV and V and $\log g = 3.5$ for luminosity class III. The uncertainty in the derived temperature is ± 2000 K around 30000 K and 700 K around 10000 K. The values of

the derived temperatures are listed in Table 3. In Table 3 we have also included seven Be stars for which the continuum energy distribution curves were taken from Schild (1976). For these Be stars the effective temperatures estimated are those corresponding to their spectral types (Bohm–Vitense 1981). The uncertainty in the effective temperature for these stars is ±5 per cent.

4 The observed Balmer excess and Paschen excess

The size of the Balmer discontinuity is, in fact, the quantity most easily derivable from photometry, since it is nearly independent of reddening. There have been debates over the proper way to measure the size of the discontinuity (Mihalas 1966). In the present investigation the Balmer continua and Paschen continua were simply extrapolated linearly to 2.70 μm^{-1} (λ3600 Å) and the difference in magnitudes was defined as the Balmer discontinuity, D_B. Scatter in the data was the major source of error in the extrapolation of the Balmer continuum. Table 3 lists the values of Balmer jumps for the programme Be stars along with a number of other relevant stellar parameters. The spectral types for most of the stars are from Jaschek *et al.* (1980). The visual magnitudes are taken from Hirshfeld & Sinnott (1982).

The qualitative impression of a small Balmer jump in the Be stars of the present study is confirmed in Fig. 1, where the observed discontinuity for each star is plotted as a function of the stellar temperature. Also shown in Fig. 1 is the theoretical relation for log g=4.0 and log g=3.5, taken from the models of Kurucz (1979). Fig. 1 shows that the size of D_B for a large fraction of Be stars is much smaller than that for normal main-sequence stars. It is also evident that the effect is too large to be caused by observational error or gravity effects. Thus, a smaller than normal discontinuity seems to be a general feature of Be stars. A similar phenomenon has also been noted in the observations of the classical Be stars (Schild *et al.* 1974). The Balmer excess, ΔD_B, defined as the magnitude difference between theoretical and observed values of D_B, was derived from Fig. 1 and is listed in Table 3.

In the Paschen continuum, an additional problem was the choice of points by which to define the continuum; since the slope is not constant over the range of observed wavelengths. To minimize the effect of observational errors in the calculation of Paschen excess emission, it is therefore advisable to use observations at the longest wavelength available. Therefore, the Paschen excess was measured at 1.25 μm^{-1} (λ8000 Å). The difference in magnitude between the observed continuum and the fitted theoretical continuum at 1.25 μm^{-1} is defined as the Paschen excess, Δm_{IR}. The values of the Paschen excess for the programme stars are listed in the last column of Table 3.

5 Quantitative determination of the excess emission measures, ε

5.1 BALMER EXCESS

It is well known that Be stars possess circumstellar envelopes which give rise to emission lines, infrared excess, ultraviolet excess and polarization, etc. Not all these effects need arise in the same region of the envelope; but they do suggest that there is extensive matter surrounding the star, which could be ionized or neutral. It is, therefore, natural to associate the excess radiation in the Balmer continuum and Paschen continuum with the circumstellar envelope. As has been suggested by Garrison (1978), let us assume that the Balmer excess may be most likely due to free–bound emission in the Balmer continuum of hydrogen atoms in an ionized or predominantly ionized region near the star. Therefore, the radiation emitted in the circumstellar envelope would increase the stellar flux shortward of the Balmer jump, thereby decreasing the observed Balmer discontinuity.

Let us consider the optically thin case of the Be star envelope. The Balmer excess, ΔD_B, is just the ratio of the flux from the star shortward of the Balmer jump to the combined flux from the star plus the circumstellar envelope:

$$\Delta D_B = -2.5 \log \frac{4\pi R_*^2 \pi F_\nu}{4\pi R_*^2 \pi F_\nu + 4\pi \int_{V_s} j_{\nu fb} \, dV_s}, \tag{1}$$

where R_* is the radius of the star, F_ν is the flux from the star shortward of the Balmer discontinuity (erg cm^{-2} s^{-1}), $j_{\nu fb}$ is the volume emission coefficient for the free–bound H transition (erg cm^{-3} s^{-1} sr^{-1} Hz^{-1}) and V_s is the volume of the emitting region.

Table 2. (a) Colour excess of the programme Be stars.

Sl. No.	Star name	HR	HD	E(B–V)	A_V
1		1204	24479	0.00	0.000
2		1305	26670	0.02	0.065
3		1763	34989	0.06	0.195
4		1820	35912	0.06	0.195
5		2418	47054	0.02	0.065
6	27 CMa	2745	56014	0.00	0.000
7	oPup	3034	63462	0.15	0.488
8	χ Oph	6118	148184	0.30	0.975
9		6873	168797	0.07	0.228
10		6881	169033	0.10	0.325
11		6984	171780	0.03	0.098
12	ES Vul	7318	180968	0.16	0.520
13		7403	183362	0.04	0.130
14	β² Cyg	7418	183914	0.02	0.065
15	k Aql	7446	184915	0.18	0.585
16		7983	198625	0.06	0.195
17	59 Cyg	8047	200120	0.05	0.163
18	νCyg	8146	202904	0.05	0.163
19	31 Peg	8520	212076	0.08	0.260

5

Table 2. (b) Dereddened continuum energy distribution data of the observed Be stars normalized to wavelength λ5500 Å.

Wavelength (Å)	1/λ (μm⁻¹)	HR 1204	HR 1305	R.C.	HR 1763	R.C.	HR 1820	R.C.	HR 2418	R.C.	HR 2745
		m	m	m	m	m	m	m	m	m	m
3200	3.13	0.754	0.217	0.175	-0.750	0.520	-0.573	0.520	0.300	0.175	-0.225
3300	3.03	0.714	0.193	0.170	-0.704	0.502	-0.508	0.502	0.299	0.170	-0.198
3400	2.94	0.730	0.198	0.165	-0.658	0.488	-0.425	0.488	0.351	0.165	-0.170
3500	2.86	0.710	0.155	0.160	-0.598	0.472	-0.404	0.472	0.315	0.160	-0.181
3600	2.78	0.687	0.145	0.155	-0.524	0.455	-0.412	0.455	0.304	0.155	-0.146
3700	2.70	0.620	0.132	0.150	-0.475	0.440	-0.363	0.440	0.330	0.150	-0.130
3800	2.63	0.170	-0.190	0.145	-0.510	0.425	-0.500	0.425	-0.200	0.145	-0.336
3900	2.56	-0.250	-0.425	0.140	-0.570	0.410	-0.540	0.410	-0.375	0.140	-0.470
4000	2.50	-0.299	-0.420	0.132	-0.546	0.392	-0.500	0.392	-0.385	0.132	-0.468
4100	2.44	-0.340	-0.387	0.130	-0.500	0.380	-0.485	0.380	-0.364	0.130	-0.426
4200	2.38	-0.327	-0.362	0.125	-0.463	0.367	-0.447	0.367	-0.334	0.125	-0.397
4300	2.33	-0.306	-0.335	0.120	-0.423	0.355	-0.402	0.355	-0.315	0.120	-0.375
4400	2.27	-0.257	-0.316	0.115	-0.391	0.340	-0.360	0.340	-0.277	0.115	-0.342
4500	2.22	-0.230	-0.275	0.110	-0.340	0.327	-0.364	0.327	-0.245	0.110	-0.293
4600	2.17	-0.204	-0.257	0.105	-0.300	0.312	-0.302	0.312	-0.225	0.105	-0.271
4700	2.13	-0.195	-0.230	0.100	-0.276	0.300	-0.257	0.300	-0.210	0.100	-0.224
4800	2.08	-0.170	-0.181	0.098	-0.224	0.287	-0.239	0.287	-0.165	0.098	-0.214
4900	2.04	-0.137	-0.165	0.092	-0.209	0.272	-0.187	0.272	-0.159	0.092	-0.127
5000	2.00	-0.118	-0.137	0.090	-0.155	0.260	-0.160	0.260	-0.120	0.090	-0.138
5100	1.96	-0.100	-0.106	0.082	-0.138	0.245	-0.140	0.245	-0.096	0.082	-0.126
5200	1.92	-0.083	-0.090	0.080	-0.103	0.230	-0.090	0.230	-0.060	0.080	-0.077
5300	1.89	-0.046	-0.044	0.075	-0.051	0.220	-0.062	0.220	-0.034	0.075	-0.012
5400	1.85	-0.028	-0.025	0.070	-0.038	0.205	-0.042	0.205	-0.029	0.070	-0.019
5500	1.82	0.000	0.000	0.065	0.000	0.195	0.000	0.195	0.000	0.065	0.000

5600	1.79	0.030	0.035	0.062	0.037	0.185	0.018	0.185	0.040	0.062	0.033
5700	1.75	0.036	0.042	0.060	0.080	0.175	0.032	0.175	0.065	0.060	0.066
5800	1.72	0.071	0.090	0.058	0.109	0.167	0.086	0.167	0.075	0.058	0.065
5900	1.69	0.090	0.106	0.052	0.115	0.160	0.130	0.160	0.098	0.052	0.088
6000	1.67	0.100	0.130	0.050	0.163	0.150	0.157	0.150	0.129	0.050	0.110
6100	1.64	0.116	0.155	0.045	0.190	0.140	0.160	0.140	0.151	0.045	0.136
6200	1.61	0.110	0.191	0.042	0.208	0.133	0.183	0.133	0.181	0.042	0.162
6300	1.59	0.133	0.200	0.040	0.239	0.125	0.188	0.125	0.206	0.040	0.165
6400	1.56	0.125	0.226	0.038	0.245	0.120	0.193	0.120	0.237	0.038	0.180
6500	1.53	0.153	0.249	0.035	0.262	0.115	0.220	0.115	0.264	0.035	0.209
6600	1.51	0.190	0.264	0.032	0.285	0.110	0.240	0.110	0.254	0.032	0.224
6700	1.49	0.180	0.250	0.030	0.273	0.100	0.219	0.100	0.263	0.030	0.284
6800	1.47	0.202	0.285	0.030	0.299	0.092	0.248	0.092	0.275	0.030	0.294
6900	1.45	0.225	0.290	0.028	0.284	0.088	0.290	0.088	0.299	0.028	0.301
7000	1.43	0.245	0.320	0.025	0.308	0.080	0.275	0.080	0.293	0.025	0.319
7100	1.41	0.236	0.350	0.022	0.323	0.075	0.273	0.075	0.331	0.022	0.350
7200	1.39	0.257	0.365	0.022	0.355	0.070	0.296	0.070	0.319	0.022	0.353
7300	1.37	0.247	0.360	0.020	0.357	0.065	0.324	0.065	0.370	0.020	0.406
7400	1.35	0.288	0.390	0.020	0.420	0.060	0.359	0.060	0.364	0.020	0.436
7500	1.33	0.293	0.380	0.018	0.429	0.055	0.310	0.055	0.370	0.018	0.469
7600	1.32	0.325	0.414	0.016	0.450	0.050	0.424	0.050	0.398	0.016	0.476
7700	1.30	0.327	0.476	0.013	0.480	0.045	0.470	0.045	0.437	0.013	0.480
7800	1.28	0.366	0.473	0.011	0.470	0.040	0.465	0.040	0.452	0.011	0.470
7900	1.27	0.388	0.524	0.010	0.496	0.035	0.516	0.035	0.498	0.010	0.490
8000	1.25	0.413	0.550	0.010	0.500	0.030	0.558	0.030	0.520	0.010	0.492

Table 2. (b) – *continued*

Wavelength (Å)	$1/\lambda$ (μm^{-1})	HR3034 m	R.C.	HR6118 m	R.C.	HR6873 m	R.C.	HR6881 m	R.C.	HR6984 m	R.C.	HR7318 m	R.C.
3200	3.13	-0.725	1.285	–	–	-0.270	0.605	0.301	0.855	-0.086	0.255	-0.825	1.370
3300	3.03	-0.758	1.245	–	–	-0.233	0.585	0.286	0.830	-0.035	0.252	-0.727	1.330
3400	2.94	-0.750	1.200	–	–	-0.225	0.570	0.259	0.802	0.000	0.245	-0.647	1.287
3500	2.86	-0.700	1.162	-0.465	2.325	-0.183	0.550	0.299	0.780	-0.013	0.235	-0.664	1.245
3600	2.78	-0.650	1.123	-0.357	2.248	-0.142	0.532	0.290	0.750	0.025	0.230	-0.560	1.205
3700	2.70	-0.452	1.083	-0.431	2.172	-0.083	0.515	0.284	0.725	0.062	0.220	-0.525	1.163
3800	2.63	-0.501	1.050	-0.484	2.100	-0.360	0.495	-0.154	0.700	-0.331	0.210	-0.556	1.122
3900	2.36	-0.533	1.013	-0.514	2.023	-0.477	0.478	-0.356	0.675	-0.425	0.205	-0.588	1.080
4000	2.50	-0.550	0.975	-0.530	1.945	-0.480	0.460	-0.375	0.650	-0.449	0.197	-0.556	1.040
4100	2.44	-0.545	0.935	-0.485	1.875	-0.436	0.448	-0.357	0.625	-0.410	0.188	-0.512	1.005
4200	2.38	-0.480	0.900	-0.465	1.805	-0.410	0.430	-0.333	0.600	-0.380	0.180	-0.463	0.970
4300	2.33	-0.445	0.865	-0.450	1.735	-0.372	0.412	-0.310	0.580	-0.365	0.175	-0.448	0.935
4400	2.27	-0.405	0.832	-0.395	1.662	-0.345	0.398	-0.280	0.555	-0.320	0.170	-0.377	0.900
4500	2.22	-0.353	0.798	-0.365	1.595	-0.317	0.380	-0.266	0.532	-0.282	0.160	-0.318	0.865
4600	2.17	-0.333	0.763	-0.346	1.527	-0.285	0.365	-0.216	0.512	-0.270	0.150	-0.320	0.830
4700	2.13	-0.277	0.732	-0.286	1.462	-0.240	0.350	-0.198	0.488	-0.227	0.145	-0.293	0.796
4800	2.08	-0.270	0.700	-0.269	1.397	-0.210	0.335	-0.170	0.467	-0.195	0.140	-0.235	0.760
4900	2.04	-0.221	0.665	-0.212	1.335	-0.175	0.320	-0.137	0.448	-0.180	0.130	-0.200	0.725
5000	2.00	-0.180	0.633	-0.194	1.272	-0.150	0.305	-0.130	0.425	-0.133	0.120	-0.187	0.690
5100	1.96	-0.152	0.605	-0.144	1.210	-0.130	0.290	-0.094	0.405	-0.110	0.115	-0.127	0.655
5200	1.92	-0.117	0.573	-0.118	1.145	-0.070	0.272	-0.056	0.385	-0.090	0.110	-0.099	0.620
5300	1.89	-0.065	0.542	-0.102	1.085	-0.049	0.260	-0.049	0.366	-0.063	0.105	-0.067	0.585
5400	1.85	-0.055	0.515	-0.055	1.025	-0.032	0.240	-0.020	0.345	-0.020	0.100	-0.026	0.550
5500	1.82	0.000	0.488	0.000	0.975	0.000	0.228	0.000	0.325	0.000	0.098	0.000	0.520

5600	1.79	0.017	0.465	0.008	0.930	0.033	0.218	0.020	0.310	0.021	0.090	0.023	0.500
5700	1.75	0.065	0.442	0.018	0.880	0.058	0.205	0.027	0.295	0.065	0.085	0.082	0.473
5800	1.72	0.112	0.420	0.036	0.835	0.100	0.192	0.081	0.280	0.070	0.082	0.014	0.450
5900	1.69	0.135	0.393	0.082	0.790	0.105	0.180	0.110	0.263	0.120	0.080	0.124	0.422
6000	1.67	0.186	0.370	0.120	0.750	0.145	0.172	0.136	0.250	0.140	0.075	0.175	0.400
6100	1.64	0.240	0.350	0.166	0.708	0.150	0.162	0.140	0.236	0.160	0.070	0.198	0.380
6200	1.61	0.290	0.333	0.214	0.670	0.198	0.155	0.164	0.220	0.175	0.068	0.245	0.360
6300	1.59	0.320	0.312	0.230	0.630	0.201	0.147	0.157	0.210	0.198	0.062	0.265	0.340
6400	1.56	0.322	0.300	0.240	0.600	0.235	0.140	0.170	0.200	0.225	0.060	0.295	0.320
6500	1.53	0.338	0.282	0.290	0.570	0.276	0.130	0.167	0.191	0.262	0.058	0.350	0.302
6600	1.51	0.350	0.270	0.290	0.530	0.310	0.120	0.195	0.180	0.292	0.055	0.355	0.285
6700	1.49	0.349	0.250	0.335	0.505	0.311	0.115	0.180	0.168	0.306	0.052	0.369	0.267
6800	1.47	0.375	0.234	0.345	0.473	0.350	0.105	0.209	0.157	0.326	0.050	0.367	0.250
6900	1.45	0.416	0.220	0.323	0.440	0.382	0.100	0.218	0.148	0.336	0.045	0.401	0.230
7000	1.43	0.444	0.200	0.314	0.408	0.398	0.090	0.215	0.135	0.357	0.042	0.420	0.220
7100	1.41	0.496	0.185	0.297	0.370	0.430	0.087	0.232	0.125	0.380	0.040	0.419	0.200
7200	1.39	0.525	0.172	0.354	0.342	0.440	0.080	0.224	0.118	0.378	0.038	0.454	0.187
7300	1.37	0.585	0.160	0.323	0.315	0.450	0.075	0.257	0.108	0.377	0.035	0.437	0.170
7400	1.35	0.590	0.147	0.370	0.290	0.460	0.070	0.290	0.100	0.395	0.030	0.458	0.160
7500	1.33	0.620	0.133	0.376	0.263	0.499	0.065	0.330	0.090	0.427	0.028	0.515	0.147
7600	1.32	0.664	0.120	0.380	0.238	0.520	0.060	0.320	0.080	0.421	0.025	0.510	0.130
7700	1.30	0.660	0.110	0.375	0.215	0.539	0.055	0.317	0.075	0.470	0.020	0.535	0.120
7800	1.28	0.659	0.100	0.379	0.195	0.552	0.050	0.393	0.065	0.464	0.020	0.550	0.110
7900	1.27	0.653	0.090	0.378	0.172	0.529	0.045	0.435	0.060	0.473	0.018	0.585	0.100
8000	1.25	0.668	0.080	0.385	0.155	0.612	0.040	0.470	0.055	0.505	0.016	0.636	0.090

134   *P. S. Goraya*

Table 2. (b) – continued

Wave-length (Å)	$1/\lambda$ (μm⁻¹)	HR7403 m	HR7403 R.C.	HR7418 m	HR7418 R.C.	HR7446 m	HR7446 R.C.	HR7983 m	HR7983 R.C.	HR8047 m	HR8047 R.C.	HR8146 m	HR8146 R.C.	HR8520 m	HR8520 R.C.
3200	3.13	-0.450	0.345	0.430	0.175	-0.075	1.540	-0.050	0.520	-0.475	0.430	-0.475	0.430	-0.393	0.690
3300	3.03	-0.458	0.335	0.435	0.170	-0.955	1.492	-0.037	0.502	-0.685	0.420	-0.451	0.420	-0.340	0.670
3400	2.94	-0.440	0.325	0.401	0.165	-0.856	1.443	-0.070	0.488	-0.650	0.405	-0.420	0.405	-0.348	0.650
3500	2.86	-0.390	0.315	0.465	0.160	-0.809	1.395	-0.087	0.472	-0.657	0.390	-0.444	0.390	-0.355	0.630
3600	2.78	-0.370	0.305	0.464	0.155	-0.725	1.350	-0.076	0.455	-0.588	0.380	-0.427	0.380	-0.350	0.610
3700	2.70	-0.360	0.295	0.262	0.150	-0.613	1.305	-0.004	0.440	-0.450	0.365	-0.320	0.365	-0.335	0.590
3800	2.63	-0.415	0.285	-0.095	0.145	-0.594	1.257	-0.315	0.425	-0.465	0.352	-0.417	0.352	-0.348	0.565
3900	2.56	-0.532	0.275	-0.285	0.140	-0.600	1.212	-0.436	0.410	-0.554	0.300	-0.550	0.340	-0.475	0.545
4000	2.50	-0.514	0.262	-0.350	0.132	-0.516	1.170	-0.448	0.392	-0.550	0.330	-0.510	0.330	-0.506	0.520
4100	2.44	-0.474	0.255	-0.370	0.130	-0.530	1.126	-0.418	0.380	-0.500	0.315	-0.482	0.315	-0.480	0.505
4200	2.38	-0.430	0.245	-0.352	0.125	-0.487	1.085	-0.403	0.367	-0.463	0.305	-0.455	0.306	-0.425	0.485
4300	2.33	-0.410	0.235	-0.313	0.120	-0.429	1.044	-0.360	0.355	-0.420	0.285	-0.410	0.285	-0.383	0.470
4400	2.27	-0.373	0.230	-0.277	0.115	-0.407	1.002	-0.320	0.340	-0.385	0.275	-0.385	0.275	-0.369	0.450
4500	2.22	-0.325	0.220	-0.255	0.110	-0.347	0.965	-0.298	0.327	-0.342	0.265	-0.342	0.265	-0.315	0.435
4600	2.17	-0.290	0.210	-0.225	0.105	-0.325	0.922	-0.275	0.312	-0.315	0.255	-0.308	0.255	-0.274	0.417
4700	2.13	-0.270	0.200	-0.200	0.100	-0.275	0.880	-0.233	0.300	-0.280	0.245	-0.267	0.245	-0.227	0.400
4800	2.08	-0.220	0.190	-0.175	0.098	-0.234	0.842	-0.210	0.287	-0.243	0.235	-0.240	0.235	-0.239	0.380
4900	2.04	-0.206	0.180	-0.126	0.092	-0.195	0.800	-0.160	0.272	-0.200	0.220	-0.215	0.220	-0.215	0.365
5000	2.00	-0.164	0.170	-0.120	0.090	-0.161	0.765	-0.160	0.260	-0.170	0.212	-0.185	0.212	-0.148	0.347
5100	1.96	-0.130	0.165	-0.080	0.082	-0.139	0.730	-0.113	0.245	-0.130	0.205	-0.150	0.205	-0.126	0.330
5200	1.92	-0.107	0.155	-0.068	0.080	-0.109	0.690	-0.080	0.230	-0.108	0.195	-0.085	0.195	-0.092	0.310
5300	1.89	-0.045	0.145	-0.050	0.075	-0.056	0.658	-0.065	0.220	-0.017	0.180	-0.062	0.180	-0.070	0.295
5400	1.85	-0.018	0.140	-0.020	0.070	-0.043	0.620	-0.015	0.205	-0.032	0.170	-0.040	0.170	-0.020	0.275
5500	1.82	0.000	0.130	0.000	0.067	0.000	0.685	0.000	0.195	0.000	0.163	0.000	0.163	0.000	0.260

5600	1.79	0.038	0.125	0.024	0.062	0.049	0.560	0.042	0.185	0.030	0.155	0.025	0.155	0.019	0.250
5700	1.75	0.057	0.120	0.065	0.060	0.070	0.530	0.063	0.175	0.080	0.150	0.055	0.150	0.033	0.235
5800	1.72	0.099	0.110	0.064	0.058	0.096	0.500	0.077	0.167	0.120	0.142	0.090	0.140	0.059	0.220
5900	1.69	0.138	0.105	0.090	0.052	0.145	0.470	0.115	0.160	0.135	0.135	0.112	0.135	0.075	0.210
6000	1.67	0.152	0.100	0.100	0.050	0.179	0.445	0.150	0.150	0.152	0.126	0.153	0.126	0.098	0.200
6100	1.64	0.199	0.090	0.119	0.048	0.191	0.920	0.180	0.140	0.188	0.120	0.151	0.120	0.086	0.190
6200	1.61	0.205	0.085	0.132	0.042	0.222	0.400	0.184	0.133	0.212	0.110	0.150	0.110	0.121	0.177
6300	1.59	0.255	0.080	0.160	0.040	0.275	0.376	0.235	0.125	0.225	0.105	0.188	0.105	0.141	0.170
6400	1.56	0.280	0.080	0.180	0.038	0.286	0.355	0.262	0.120	0.235	0.100	0.210	0.100	0.155	0.160
6500	1.53	0.310	0.075	0.200	0.035	0.315	0.338	0.262	0.115	0.290	0.095	0.256	0.095	0.148	0.148
6600	1.51	0.315	0.070	0.220	0.032	0.354	0.320	0.276	0.110	0.336	0.090	0.255	0.090	0.182	0.140
6700	1.49	0.324	0.065	0.220	0.030	0.355	0.300	0.293	0.100	0.370	0.085	0.267	0.085	0.222	0.130
6800	1.47	0.345	0.060	0.255	0.030	0.394	0.380	0.310	0.092	0.370	0.075	0.280	0.075	0.241	0.120
6900	1.45	0.385	0.055	0.275	0.028	0.420	0.262	0.332	0.088	0.420	0.072	0.300	0.072	0.232	0.115
7000	1.43	0.385	0.052	0.283	0.025	0.440	0.250	0.320	0.080	0.402	0.070	0.339	0.070	0.281	0.110
7100	1.41	0.410	0.050	0.284	0.022	0.469	0.225	0.358	0.075	0.455	0.062	0.355	0.062	0.314	0.100
7200	1.39	0.425	0.045	0.320	0.022	0.487	0.210	0.395	0.070	0.508	0.060	0.373	0.060	0.325	0.095
7300	1.37	0.430	0.042	0.345	0.020	0.526	0.190	0.420	0.065	0.510	0.055	0.391	0.055	0.376	0.085
7400	1.35	0.475	0.040	0.370	0.020	0.527	0.172	0.418	0.060	0.500	0.052	0.394	0.052	0.361	0.080
7500	1.33	0.679	0.035	0.385	0.018	0.505	0.160	0.466	0.055	0.501	0.050	0.399	0.050	0.349	0.070
7600	1.32	0.502	0.032	0.387	0.016	0.542	0.142	0.500	0.050	0.544	0.045	0.400	0.045	0.368	0.065
7700	1.30	0.552	0.030	0.403	0.013	0.526	0.130	0.498	0.045	0.554	0.040	0.410	0.040	0.400	0.060
7800	1.28	0.551	0.025	0.405	0.011	0.622	0.120	0.530	0.040	0.539	0.037	0.420	0.037	0.390	0.053
7900	1.27	0.593	0.022	0.402	0.010	0.640	0.110	0.570	0.035	0.540	0.033	0.408	0.033	0.370	0.045
8000	1.25	0.562	0.020	0.410	0.010	0.704	0.100	0.620	0.030	0.549	0.030	0.399	0.030	0.385	0.040

Table 3. Stellar parameters, Balmer excess and Paschen excess of programme Be stars.

	Star name	HR	HD	Spectral Type MK	V	$T(K)$	$\log g$	D_B	ΔD_B	Δm_{IR}
27	γ Cas†	264	5394	B0.5 IV	2.47	29 000	4.0	0.00±0.03 mag	0.17 mag	0.15 mag
	ϕ Per†	496	10 516	B1 V	4.07	25 000	4.0	0.05	0.19	0.19
28	Tau†	1180	23 862	B8 V	5.06	12 000	4.0	0.93	0.06	0.01
		1204	24 470	B9.5 V	5.03	11 000	4.0	1.13	0.03	0.12
48	Per†	1273	25 940	B3 V	4.04	19 000	4.0	0.36	0.07	0.04
		1305	26 670	B5 Vn*	5.6	16 000	4.0	0.51	0.16	0.05
56	Eri†	1508	30 076	B2 V	5.90	21 000	4.0	0.19	0.16	0.20
105	Tau†	1660	32 991	B2 V	5.89	21 000	4.0	0.20	0.15	0.05
		1763	34 989	B1 V*	5.80	25 000	4.0	0.18	0.06	0.20
		1820	35 912	B2 V*	6.41	22 000	4.0	0.25	0.06	0.13
		2418	47 054	B3 V	5.52	13 000	4.0	0.81	0.05	0.07
27	CMa	2745	56 014	B3 III*	4.66	18 000	3.5	0.40	0.07	0.10
28	ω CMa†	2749	56 139	B2 IV–V*	3.35	22 000	4.0	0.23	0.09	0.03
	o Pup	3034	63 462	B0 Vp*	4.50	30 000	4.0	0.08	0.07	0.01
7	χ Oph	6118	148 184	B1 V	4.42	22 500	4.0	0.20	0.10	0.25
		6873	168 797	B3 Vn	6.13	18 000	4.0	0.43	0.06	0.04
		6881	169 033	B8 IV	5.7	13 000	4.0	0.76	0.10	0.10
		6984	171 780	B6 V	6.10	16 000	4.0	0.55	0.05	0.08
2	Es Vul	7318	180 968	B0.5 IV*	5.43	30 000	4.0	0.11	0.05	0.21
		7403	183 362	B2 Vn	6.34	22 000	4.0	0.28	0.04	0.05
6	β^2 Cyg	7418	183 914	B8 V	5.11	12 000	4.0	0.87	0.12	0.16
39	$\varkappa$ Aql	7446	184 915	B0.5 III*	4.95	30 000	3.5	0.01	0.10	0.05
		7983	198 625	B4 V*	6.33	17 000	4.0	0.50	0.04	0.05
59	Cyg	8047	200 120	B1	4.74	25 000	4.0	0.11	0.13	0.05
66	v Cyg	8146	202 904	B2 V	4.43	22 500	4.0	0.26	0.04	0.29
31	Peg	8520	212 076	B2 V	5.01	20 000	4.0	0.25	0.14	0.23

* Spectral types from Hoffleit (1983).

† Continuum energy distributions from Schild (1976).

Now, let us assume the photoionization of a hydrogen-like system. When the free electrons are in local thermodynamic equilibrium at temperature T_s, the velocity distribution is Maxwellian. In this case, the recombination power, $P_r(n, \nu)$, radiated per unit volume when recombining to level n is, for hydrogen-like atoms, given by (*cf.* Lang 1974):

$$P_r(n, \nu) = 4\pi j_{\nu fb} = N_e N_i \frac{Z^4 K}{(kT_s)^{3/2}} \frac{g_{fb}}{n^3} \exp\left(-\frac{h\nu}{kT_s} + \frac{Z^2 E_H}{n^2 kT_s}\right), \tag{2}$$

where $K = 3.4 \times 10^{-40} (E_H)^{3/2}$ erg$^{5/2}$ cm^3, $E_H \approx 2.2 \times 10^{-11}$ erg is the ionization energy of hydrogen, n is the principal quantum number of the bound level, N_e and N_i are the electron and ion number densities (cm^{-3}), g_{fb} is the free–bound Gaunt factor, T_s is the envelope temperature. For a hydrogen envelope $Z = 1$, therefore, equation (2) reduces to

$$4\pi j_{\nu fb} = 2.16 \times 10^{-32} \, T_s^{-3/2} \, N_e N_i \exp\left(-\frac{h\nu}{kT_s} + \frac{E_H}{n^2 kT_s}\right)\left(\frac{g_{fb}}{n^3}\right). \tag{3a}$$

For the Balmer continuum near $\lambda 3600$ Å,

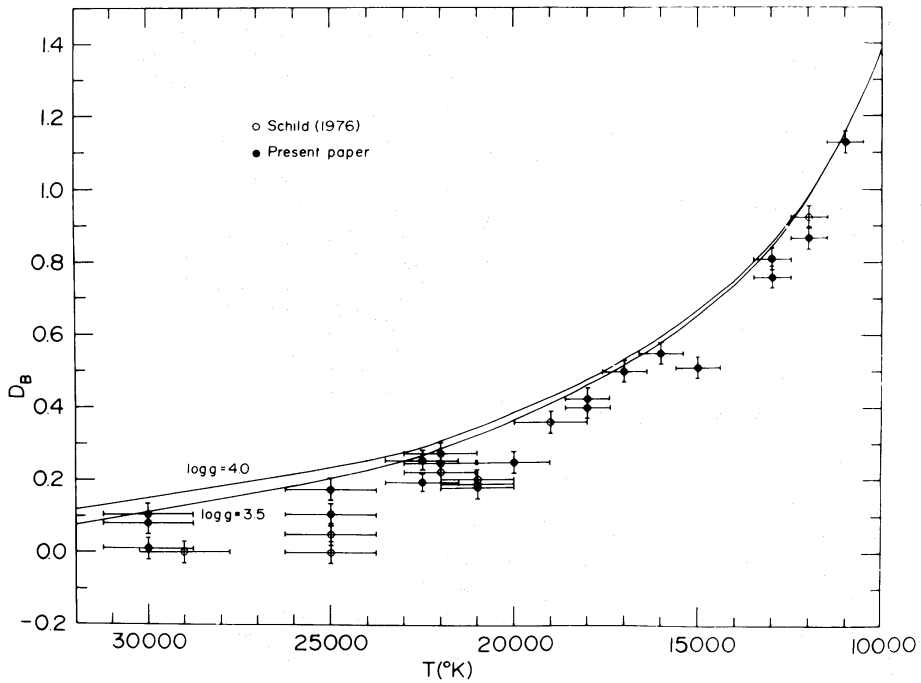$$\exp\left(-\frac{h\nu}{kT_s} + \frac{E_H}{n^2 kT_s}\right) \approx 1,$$

Figure 1. Comparison of observed Balmer jumps with the Balmer jumps from model atmospheres as a function of temperature. The vertical error bars reflect errors in spectrophotometry and uncertainty in measuring the discontinuity. The horizontal error bars reflect uncertainty in temperature due to error in spectrophotometry and uncertainty in fitting of models with observations.

$n=2(n^3=8)$, $g_{fb}=0.89$ (Allen 1976). Substituting the values of different constants, equation (3a) reduces to

$$j_{\nu fb}=1.88\times10^{-34}\,T_s^{-3/2}\,N_e N_i \text{ erg cm}^{-3}\text{ s}^{-1}\text{ sr}^{-1}\text{ Hz}^{-1}. \tag{3b}$$

Substituting the value of $j_{\nu fb}$ in equation (1) we get

$$\Delta D_B=-2.5 \log \frac{4\pi R_*^2 \pi F_\nu}{4\pi R_*^2 \pi F_\nu+4\pi \displaystyle\int_{V_s} 1.88\times10^{-34}\,T_s^{-3/2}\,N_e N_i\, dV_s} \; .$$

Or

$$\Delta D_B=-2.5 \log \frac{\pi F_\nu}{\pi F_\nu+1.88\times10^{-34}\,T_s^{-3/2}\left(\displaystyle\int_{V_s} N_e N_i\, dV_s\right)R_*^{-2}}. \tag{4}$$

For convenience, defining an emission measure, ε, by

$$\varepsilon = \frac{\left(\displaystyle\int_{V_s} N_e N_i\, dV_s\right)}{R_*^2}$$

and substituting in equation (4), we get

$$\Delta D_B=-2.5 \log \frac{\pi F_\nu}{\pi F_\nu+1.88\times10^{-34}\,T_s^{-3/2}\varepsilon}.$$

Rearranging the above equation we obtain

$$\varepsilon_{UV} = 1.67 \times 10^{34} F_\nu T_s^{3/2} [\text{dex} (0.4 \, \Delta D_B) - 1]. \tag{5}$$

Thus, the Balmer emission measure, ε_{UV}, can be computed from the observed Balmer excess, ΔD_B, for any value of the envelope temperature, T_s. It is also necessary to assume a stellar temperature, T, to obtain the flux, F_ν, from the model atmospheres. This approach requires no knowledge of the distance to the object.

5.2 PASCHEN EXCESS

The ionized circumstellar envelope producing the Balmer excess might also be expected to produce excess radiation in the near-infrared region near the Paschen discontinuity. Indeed, it was noted that in many Be stars, the observed continuum did lie above the expected stellar-model continuum after the reddening correction was made. The most widely accepted explanation for such infrared excess emission in Be stars is the free–bound and free–free emission originating in the ionized circumstellar envelope (Gehrz et al. 1974; Scargle et al. 1978). With the use of an emission measure necessary to produce the observed Balmer excess one can predict the Paschen excess due to Paschen free–bound and also free–free emission.

For comparison with observations, the magnitude excess above the stellar continuum should be computed. The Paschen excess Δm_{IR} is simply the ratio of the flux from the star at some point in the infrared region to the combined flux from the star plus the circumstellar envelope:

$$\Delta m_{IR} = -2.5 \log \frac{4\pi R_*^2 \pi F_{\nu *}}{4\pi R_*^2 \pi F_{\nu *} + 4\pi \int_{V_s} J_{\nu fb+ff} \, dV_s} \tag{6}$$

where the symbols have the same meaning as in equation (1), except that $F_{\nu *}$ is now at some point in the Paschen continuum. The free–bound contribution in the Paschen continuum can be computed from equation (3a), with $n = 3$, $g = 0.92$ (Allen 1976),

$$\exp\left(-\frac{h\nu}{kT_s} + \frac{E_H}{n^2 kT_s}\right) \approx 1;$$

and is given by

$$j_{\nu fb} = 5.657 \times 10^{-35} T_s^{-3/2} N_e N_i \text{ erg cm}^{-3} \text{ s}^{-1} \text{ sr}^{-1} \text{ Hz}^{-1}. \tag{7}$$

The free–free (Bremsstrahlung) contribution in the Paschen continuum can be given by (Allen 1976):

$$j_{\nu ff} = 5.443 \times 10^{-39} Z^2 g_{ff} \exp(-c_2/\lambda/T_s) T_s^{-1/2} N_e N_i, \tag{8}$$

where $c_2 = (h\nu/k) \approx 1.44$ is the second radiation constant. Now for the near-infrared region, $g = 0.92$ (Allen 1976) and $Z = 1$ for hydrogen; therefore equation (8) becomes

$$j_{\nu ff} = 4.953 \times 10^{-39} \exp\left(-\frac{1.44 \times 10^{-4} \lambda^{-1}}{T_s}\right) T_s^{-1/2} N_e N_i \tag{9}$$

where λ^{-1} is the inverse wavelength in μm.

So combining equations (7) and (9) into equation (6) and introducing the emission measure, ε,

Table 4. Balmer and Paschen emission measures.

HR	T_s(K)	ΔD_B	F_ν † (erg s⁻¹ cm⁻² Hz⁻¹)	ε_{UV} † (erg s⁻¹)	Δm_{IR}	$F_{\nu *}$ † (erg s⁻¹ cm⁻² Hz⁻¹)	ε_{IR} † (erg s⁻¹)	$\varepsilon_{UV}/\varepsilon_{IR}$
264	20 000	0.17	2.400 E-3	1.861 E 37	0.15	7.078 E-4	1.110 E 37	1.7
496	14 000	0.19	1.492 E-3	7.667 E 36	0.19	5.456 E-4	9.346 E 36	0.8
1180	10 000	0.06	1.733 E-4	1.644 E 35	0.01	1.799 E-4	8.737 E 34	1.9
1204	10 000	0.03	1.232 E-4	5.764 E 34	0.12	1.556 E-4	8.737 E 35	0.1
1273	14 000	0.07	7.320 E-4	1.349 E 36	0.04	3.530 E-4	1.034 E 36	1.3
1305	10 000	0.16	3.636 E-4	9.641 E 35	0.05	2.517 E-4	6.961 E 35	1.4
1508	14 000	0.16	1.050 E-3	4.457 E 36	0.20	3.938 E-4	6.539 E 36	0.7
1660	14 000	0.15	1.050 E-3	4.150 E 36	0.05	3.938 E-4	1.524 E 36	2.7
1763	14 000	0.06	1.492 E-3	2.345 E 36	0.20	5.456 E-4	9.881 E 36	0.2
1820	14 000	0.06	1.102 E-3	1.732 E 36	0.13	4.350 E-4	4.649 E 36	0.4
2418	10 000	0.05	2.316 E-4	1.637 E 35	0.07	2.041 E-4	6.879 E 35	0.2
2745	14 000	0.07	6.247 E-4	1.066 E 36	0.10	3.303 E-4	2.422 E 36	0.4
2749	14 000	0.09	1.070 E-3	2.410 E 36	0.03	4.350 E-4	1.024 E 36	2.4
3034	20 000	0.07	2.623 E-3	8.251 E 36	0.01	7.491 E-4	3.481 E 36	2.4
6118	14 000	0.10	1.116 E-3	2.885 E 36	0.25	4.570 E-4	1.005 E 37	0.3
6873	14 000	0.06	6.063 E-4	8.715 E 35	0.04	3.258 E-4	9.293 E 35	0.9
6881	10 000	0.10	2.316 E-4	3.537 E 35	0.10	2.041 E-4	1.076 E 36	0.3
6984	14 000	0.05	4.382 E-4	5.130 E 35	0.08	2.760 E-4	1.512 E 37	0.3
7318	20 000	0.05	2.623 E-3	5.243 E 36	0.21	7.491 E-4	1.725 E 37	0.3
7403	14 000	0.04	1.102 E-3	9.487 E 35	0.05	4.350 E-4	1.723 E 36	0.6
7418	10 000	0.12	1.733 E-4	3.234 E 35	0.16	1.799 E-4	1.499 E 36	0.2
7446	20 000	0.10	2.434 E-3	1.109 E 37	0.05	7.898 E-4	4.018 E 36	2.8
7983	14 000	0.04	5.220 E-4	4.731 E 35	0.05	3.009 E-4	1.048 E 36	0.5
8047	14 000	0.13	1.492 E-3	5.250 E 36	0.05	5.456 E-4	2.304 E 36	2.3
8146	14 000	0.04	1.116 E-3	1.070 E 36	0.23	4.570 E-4	1.165 E 37	0.1
8520	14 000	0.14	8.077 E-4	2.954 E 36	0.23	3.801 E-4	7.004 E 36	0.4

$X\ Ey \equiv X \times 10^y$

as defined earlier, we obtain

$$\Delta m_{IR} = -2.5 \log \frac{\pi F_{\nu *}}{\pi F_{\nu *} + \varepsilon\{5.657 \times 10^{-35} T_s^{-3/2} + 4.953 \times 10^{-39} \exp\left[-(1.44 \times 10^{-4} \lambda^{-1}/T_s)\right] T_s^{-1/2}\}}.$$

Rearranging the above equation, we get

$$\varepsilon_{IR} = \frac{10^{35} T_s^{1/2} \pi F_{\nu *}[\text{dex }(0.4\ \Delta m_{IR}) - 1]}{\{(5.657/T_s) + 4.953 \times 10^{-4} \exp\left[-(1.44 \times 10^{-4} \lambda^{-1}/T_s)\right]\}}.$$

Thus the Paschen emission measure, ε_{IR}, can be computed from the observed Paschen excess, Δm_{IR}, for any value of envelope temperature, T_s. It should be noted that as in equation (5) for the Balmer excess, the envelope temperature, T_s, is a free parameter.

By using equations (5) and (10) the Balmer and Paschen emission measures have been computed and are listed in Table 4. The assumed values of the envelope temperature, T_s, used in our calculations are listed in second column of Table 4.

In Table 4 are also listed the fluxes F_ν and $F_{\nu *}$ obtained from the model atmospheres (Kurucz 1979) representing the stellar temperature.

5.3 ON THE VALUES OF T_s

The envelope temperature, T_s, probably lies between 10 000 K and the stellar temperature, T. If the ionized region were much cooler than 10^4 K, one would expect to observe a strong free–bound
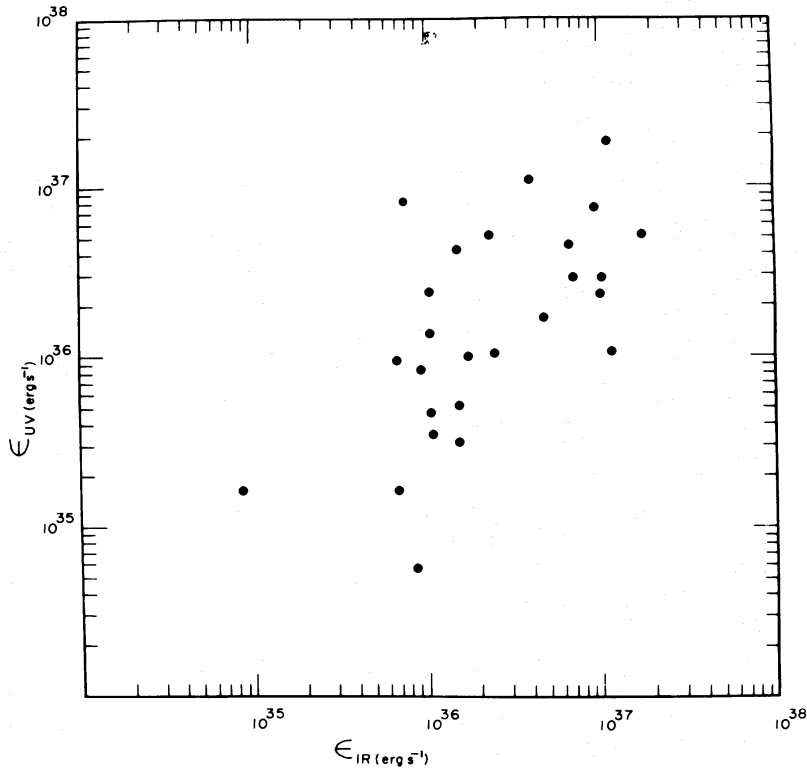
Figure 2. The Balmer emission measure, ε_{UV}, of circumstellar envelopes of Be stars as a function of Paschen emission measure, ε_{IR}.

continuum in the $\lambda\lambda 0.3$–2μm region caused by recombination of the H^- ion (Milkey & Dyck 1972; Humphreys 1974). There is, to our knowledge, no evidence of such a continuum in any Be star. Also, unless turbulent heating is present, T_s can not exceed the stellar temperature (Gehrz *et al.* 1974). Therefore, in applying equation (5) and (10) to our data, the envelope temperatures were assumed in the range $10^4 \leqslant T_s \leqslant T$. We adopted the following criteria for assuming different values of T_s:

$T_s = 20\,000$ K for $T \geqslant 25\,000$ K

$T_s = 14\,000$ K for $15\,000$ K $\leqslant T \leqslant 25\,000$ K

$T_s = 10\,000$ K for $T \leqslant 15\,000$ K

6 Correlation of near-ultraviolet excess emission with near-infrared excess emission

In Be stars the ultraviolet excess and infrared excess emission originate in the same circumstellar envelope. As a result, it is interesting to investigate if any correlation exists between the ultraviolet excess radiation and infrared excess radiation. To investigate such a correlation the Balmer and Paschen emission measures listed in Table 4 are displayed in Fig. 2. It is obvious from Fig. 2 that a poor correlation exists between the two. This result from the present investigation is contrary to the conclusions of Feinstein (1982), that no correlation exists between these two. Fig. 2 shows that there is a loose correspondence between ε_{UV} and ε_{IR}.

To understand the physical processes responsible for the observed correlation between ε_{UV} and ε_{IR} equations (5) and (10) should be examined. Comparison of equation (5) with equation (10) shows that both ε_{UV} and ε_{IR} have nearly the same functional dependence on T_s apart from the weak dependence on F_ν or $F_{\nu*}$. Consequently, the existence of some correlation between ε_{UV} and ε_{IR} is understandable.

From Table 4, it is seen that the average value of the observed ratio $\varepsilon_{UV}/\varepsilon_{IR}$ is ∼1. The observed value of $\varepsilon_{UV}/\varepsilon_{IR}$ shows that the effective emitting volumes are probably equal.

References

Allen, C. W., 1973. *Mon. Not. R. astr. Soc.*, **161**, 145.
Allen, C. W., 1976. *Astrophysical Quantities*, Athlone Press, London.
Ashok, N. M., Bhatt, H. C., Kulkarni, P. V. & Joshi, S. C., 1984. *Mon. Not. R. astr. Soc.*, **211**, 471.
Barbier, D. & Chalonge, D., 1941. *Ann. Astrophys.*, **4**, 30.
Bhatt, H. C., Ashok, N. M., Chandrasekhar, T. & Goraya, P. S., 1984. *Astr. Astrophys. Suppl.*, **58**, 685.
Blanco, V. M., Demers, S., Douglass, G. G. & FitzGerald, M. P., 1968. *Photoelectric Catalogue*, **21**, United States Naval Observatory, Washington.
Bohn.Vitense, E., 1981. *Ann. Rev. Astr. Astrophys.*, **19**, 303.
Briot, D., 1978, *Astr. Astrophys.*, **66**, 197.
Dachs, J. & Wamsteker, W., 1982. *Astr. Astrophys.*, **197**, 240.
Erro, B. I., 1969. *Bol. Obs. Ton. v Tac.*, **5**, 89.
Feinstein, A., 1968. *Zf. Astrophys.*, **68**, 29.
Feinstein, A., 1982. *IAU Symp.*, **98**, 235.
Feinstein, A. & Marraco, H. G., 1981. *Publs astr. Soc. Pacif.*, **93**, 110.
Garrison, L. M., 1978. *Astrophys. J.*, **224**, 535.
Gehrz, R. D., Hackwell, J. A. & Jones, T. W., 1974. *Astrophys. J.*, **191**, 675.
Goraya, P. S., 1980. *Astrophys. Space Sci.*, **73**, 319.
Goraya, P. S., 1981. *Astrophys.. Space Sci.*, **78**, 419.
Goraya, P. S., 1984a, *Astr. Astrophys.*, **138**, 19.
Goraya, P. S., 1984b, *Astrophys. Space Sci.*, **105**, 323.
Goraya, P. S., 1985. *Mon. Not. R. astr. Soc..*, **215**, 265.
Goraya, P. S. & Rautela, B. S., 1985. *Astrophys. Space Sci.*, **113**, 373.
Hirshfeld, A. & Sinnott, R. W., 1982. *Sky Catalogue 2000.0, 1*, Cambridge University Press.
Hoffleit, D. 1983. *The Bright Star Catalogue*, Yale University Observatory, New Haven.
Humphreys, R. M., 1974. *Astrophys. J.*, **188**, 75.
Jaschek, M., Hubert-Delplace, A. M., Hubert, H. & Jaschek, C., 1980 *Astr. Astrophys. Suppl.*, **42**, 103.
Johnson, H. L., 1967. *Astrophys. J.*, **150**, L39.
Johnson, H. L. & Morgan, W. W., 1953. *Astrophys. J.*, **117**, 313.
Kurucz, R. L., 1979. *Astrophys. J. Suppl.*, **40**, 1.
Lang, K. R., 1974. *Astrophysical Formulae*, Springer-Verlag. Berlin.
Llorente de Andres, F., Munoz, F., Lopez Arroyo, M. & Morales, C., 1981. *Astr.Astrophys.*, **98**, 418.
Lucke, P. B., 1980. *Astr. Astrophys.*, **90**, 350.
Mendoza, E. E., 1958. *Astrophys. J.*, **128**, 207.
Mihalas, D., 1966. *Astrophys. J. Suppl.*, **13**, 1.
Milkey, R. W. & Dyck, H. M., 1973. *Astrophys. J.*, **181**, 833.
Moffat, A. F. J. & Schmidt-Kaler, Th., 1976. *Astr. Astrophys.*, **48**, 115.
Neto, A. D. & de Freitas Pacheco, J. A., 1982. *Mon. Not. R. astr. Soc.*, **198**, 659.
Scargle, J. D., Erickson, E. F., Whitteborn, F. C. & Strecker, D. W., 1978. *Astrophys. J.*, **224**, 527.
Schild, R. E., 1976. *IAU Symp.*, **70**, 107.
Schild, R. E., 1977. *Astr. J.*, **82**, 337.
Schild, R. E., 1978. *Astrophys. J. Suppl.*, **37**, 77.
Schild, R. E., Chaffee, F., Frogel, J. A. & Persson, S. E., 1974. *Astrophys. J.*, **190**, 73.
Tug, H., White, N. M. & Lockwood, G. W., 1977. *Astr. Astrophys.*, **61**, 679.
Woolf, N. J., Stein, W. A. & Strittmatter, P. A., 1970. *Astr. Astrophys.*, **9**, 252.